Pergamon

Int. J. Heat Mass Transfer. Vol. 41, Nos 4–5, pp. 811–816, 1998

0017–9310/98 $19.00+0.00

PII: S0017-9310(97)00169-5

Effect of fence thickness on pressure drop and heat transfer in a perforated-fenced channel

JENN JIANG HWANG and TONG YU LIA

Department of Mechanical Engineering, Chung-Hua University, Hsinchu, Taiwan 30067, Republic of China

and

TONG-MIIN LIOU

Department of Power Mechanical Engineering, National Tsing-Hua University, Hsinchu, Taiwan 30043, Republic of China

(*Received* 30 *November* 1996 *and in final form* 28 *April* 1997)

INTRODUCTION

This note is concerned with the heat transfer/performance in a channel with perforated fences which may be used in the application of large-scale heat exchangers. The problem of this subject was introduced by Tanasawa and his coworkers [1, 2] about 15 years ago. They used the resistance-heating and thermocouple techniques to determine the heat transfer coefficients in a rectangular channel where perforated fence-turbulators were symmetrically mounted on two opposite walls. Comparisons of the thermal performance made between the three types of turbulence promoters, namely, solid, perforated and slit types, revealed that surfaces with perforated turbulence promoters performed the best. In addition, the half-perforated turbulence promoters with perforations on the lower half part of the fence provided a better thermal performance than the fully perforated turbulence promoters. Recently, Hwang and Liou [3–5] systematically investigated the effects of fence spacing, fence height, fence arrangement and fence open-area ratio on the heat transfer performance in a perforated-fenced channel. The major findings were (1) local heat transfer deterioration that occurred just behind the solid fence could be removed by perforating the fence to be permeable, (2) the thermal performance in the permeable-fenced channel was better than that in the solid-fenced one, and (3) the fence permeability was a function of the fence open-area ratio and flow Reynolds number, but independent of the fence spacing, fence height, and fence arrangement.

As listed in Table 1, the present work is an extension of the author's previous works, and continuously the effect of the fence thickness on the heat transfer and pressure drop is investigated experimentally. To the author's best knowledge, the experimental study concerning the influence of thickness-to-height ratio on the thermal–hydraulic performance is rather sparse for the channel with solid-fenced walls, let alone the channel with perforated-fenced walls. As a result, empirical prediction methods are not available to evaluate the effect of fence thickness on the heat transfer and friction for the perforated-fenced channels, which therefore constitutes a concrete motivation of the present work.

EXPERIMENT

The experiments were performed in an open-loop airflow system that consists of a settling chamber, a nozzle-like entrance, a test section, and a flow meter. A centrifugal blower driven by a 5 hp electric motor delivers air to the flow loop. The rate of mass flow of air through the flow loop is controlled by an inverter. The test section is a 1.5 m long, 4×16 cm rectangular channel constructed of two 6-mm thick aluminum plates and two 5-mm thick Plexiglas plates. The perforated fences made of aluminum bar are attached staggeringly to the two opposite aluminum plates with silicon rubber adhesive. The fence angle-of-attack is 90 degrees. Thermofoils of thickness 0.18 mm are adhered uniformly between the aluminum plate and a 6-mm-thick fiberglass board to ensure good contact. Two pieces of balsa wood (20-mm in thickness) are used to prevent heat loss from the upper and lower sides of the heated plates. The test section is instrumented with 28 copper–constantan thermocouples along the spanwise centerline of the heated plate and fences for wall temperature measurements. The junction-beads (about 0.15-mm in diameter) are carefully embedded into the wall, and then ground flat to ensure that they are flush with surfaces. The emf signals through the thermocouple wires are transferred to a hybrid recorder, and all data are then sent to a personal computer via Multi-I/O interface. As for the pressure drop measurement, the bottom heated plates of the test section is replaced by a Plexiglas plate. A total of 18 pressure taps is installed on the spanwise centerline of the Plexiglas plate for the local wall static pressure measurements. The pressure drop across the fenced walls is, therefore, measured under the adiabatic conditions. A micro-differential transducer with an accuracy of 0.02 mm water column measured the pressure differences between the static pressure taps. The fence permeability is determined by laser holographic interferometer which has been described in detail elsewhere [3], and is not elaborated on here. As given in Table 1, the fence height-to-channel hydraulic diameter and fence pitch-to-height ratios are fixed at 0.081 and 10, respectively, to facilitate the comparison with the previous results [5, 6]. The fence thickness-to-height ratio is varied from 0.16 to 0.70. At each fence thickness-to-height ratio, the fence open-area ratio is varied from 0 to 0.44. The Reynolds number (based on the duct hydraulic diameter and bulk mean velocity) for each fence configuration is ranged from 8000 to 50 000. The data are taken at the region about 10–12 hydraulic diameters downstream the test section entrance, where the spatially hydrodynamic and thermal periodicity is achieved [6].

Table 1. Fence geometry in this and previous studies

Investigations	Fenced-wall configuration	h/De	Pi/h	β	w/h
This study	Two opposite fenced walls Staggered	0.081	10	10%, 22% 38%, 44%	0.16, 0.35 0.50, 0.70
[3]	Single fenced wall	0.081 0.162	5, 10	10%, 22% 38%, 44%	1.0
[4]	Two opposite fenced walls In-line	0.063 0.081	10	10%, 22% 38%, 44%	1.0
[5]	Two opposite fenced walls Staggered	0.081 0.162	10, 15, 20	0, 50%	0.78

w = fence thickness; h = fence height; De = channel hydraulic diameter; Pi = fence spacing; β = fence open-area ratio (ratio of the perforations area to the fence frontal area).

The local pressure drag coefficient is defined as the ratio of the wall static pressure drop to fluid dynamic pressure as $C_D = (P_x - P_0)/(\rho U^2/2)$, where P_0 is the reference pressure and is taken to be the value of the first tap, and, P_x, the static wall pressure at the axial position X. Fanning friction factor for the fully-developed flow is determined by measuring the pressure gradient across the flow channel ($\Delta P/\Delta L$) and mean velocity (U). of the air, and is expressed as $f = [(-\Delta P/\Delta L)De]/(\rho U^2/8)$. The maximum uncertainties of C_D and f are estimated to be less than 7.1 and 7.3%, respectively, for the range of Reynolds number investigated by using the uncertainty estimation method of Kline and McClintock [7]. The average Nusselt number of the heated surface is defined by $\overline{Nu} = q_{net}De/[A(T_w - T_b)\ k_f]$. q_{net} represents the net convective heat transfer rate from the heated fenced wall to the coolant, and is calculated by subtracting the total heat losses from the supplied electrical power. The total heat losses include the conduction heat loss through the fiberglass insulation, the axial conduction heat loss, and the radiation heat loss. To confirm the energy conservation in the experiments, the convective heat transfer rate from the heated plates to the channel coolant is checked with the cooling air enthalpy rise along the test duct. A very good agreement in q_{net} is found between these two methods. The maximum uncertainty of the Nusselt number evaluated by the method of Kline and McClintock [7] is less than 8.2% for Reynolds number larger than 8000. Thermal performance evaluation under the constraint of the constant pumping power is widely used in the application of a variety of heat exchangers. To implement this case, the pumping power (PP) required to drive a flow rate (m) through a pressure drop (ΔP) should be noted as $PP = m\Delta P/\rho$. For a fenced channel and a smooth channel having equal hydraulic diameters and lengths, the constraint of equal pumping power can be reduced to $(f\ Re^3)_{\text{fenced channel}} = (f\ Re^3)_{\text{smooth channel}}$. Therefore, the thermal performance on the constant pumping constraint is readily to be presented by the relation between the ratios of $\overline{Nu}/\overline{Nu}_s^*$ and $f^{1/3} \cdot Re$ [5], where $\overline{Nu}_s^*$ is the average Nusselt number for a smooth channel with the flow rate at which the pumping power is the same as that obtained in the fenced channel. In this work, the friction factor of the smooth channel is given by the Blasius correlation for the fully developed circular tube flow. The maximum uncertainty of $\overline{Nu}^*$ is less than 9.2% by the estimating method of Kline and McClintock [7].

RESULTS AND DISCUSSION

Permeability limit

Some examples of the finite-fringe interferograms for flow over the perforated-fenced surfaces of various fence thicknesses are given in Fig. 1, by which the fence permeability could be judged. General tendency concluded from the interferometric fringes is that the saw-shaped fringes behind the fence mean that the fence is permeable; otherwise it is impermeable [3]. It is observed that at fixed geometric and flow parameters of $\beta = 0.22$ and $Re = 12\,000$, i.e. from Fig. 1(a)–(e), the thinner fence seems to have the higher permeability. In addition, comparison of Figs 1(d) and (f) reveals that, at a fixed fence geometry of $\beta = 0.22$, and $w/h = 0.5$, the higher flow Reynolds number allows easily the fence to be permeable. In accordance with the interferometry observation, the permeability of the perforated fence of various thicknesses is obtained, which is shown in Fig. 2 by the relation between the critical Reynolds number of initiation of flow permeability and the fence open-area ratio. The solid curves with different symbols represent the permeability limits of different fence thickness-to-height ratios. Physically, the permeability limit is a criterion for the change of the flow patterns. It is seen from this figure that the permeable zone is found to be in the region of higher fence open-area ratios and higher Reynolds numbers. The permeability limit decreases with the decrease of the fence thickness-to-height ratio. That is, at a fixed fence open-area ratio, the critical Reynolds number for initiation of flow permeability decreases with the decrease in the fence thickness-to-height ratio.

To further examine the flow permeability, the static-wall-pressure distributions are measured and shown by the local drag coefficient (C_D) distributions along the normalized axial distance X/h in Fig. 3. Because the effect of the fence thickness-to-height ratio on C_D is negligible for the solid-fenced geometry, the results of C_D of various fence thicknesses are correlated by a single curve as given in Fig. 3. The pressure drop across the solid fence is mainly contributed by the fence form drag, which is, as expected, nearly independent of the fence thickness in the range of fence thickness investigated [8]. At $\beta = 10\%$, the C_D distribution along the perforated-fence wall is similar to that along the solid-fenced wall (solid curve) except for the thinnest fence ($h/w = 0.16$). Due to the lower form drag accompanied by the permeable rib, the C_D distribution for $h/w = 0.16$ is more even than those of the other wider fences. At $\beta = 22\%$, not only the data for $h/w = 0.16$, but also those for $h/w = 0.35$ are apart from the solid curve. At the larger fence open-area ratios, say $\beta = 38$ and 44%, almost all data fall in another similar distribution, which is flatter than the solid curve because of the smaller form drag.

Heat transfer, friction and performance

The effect of fence thickness on the average Nusselt number and friction factor of the perforated-fenced wall for vari-

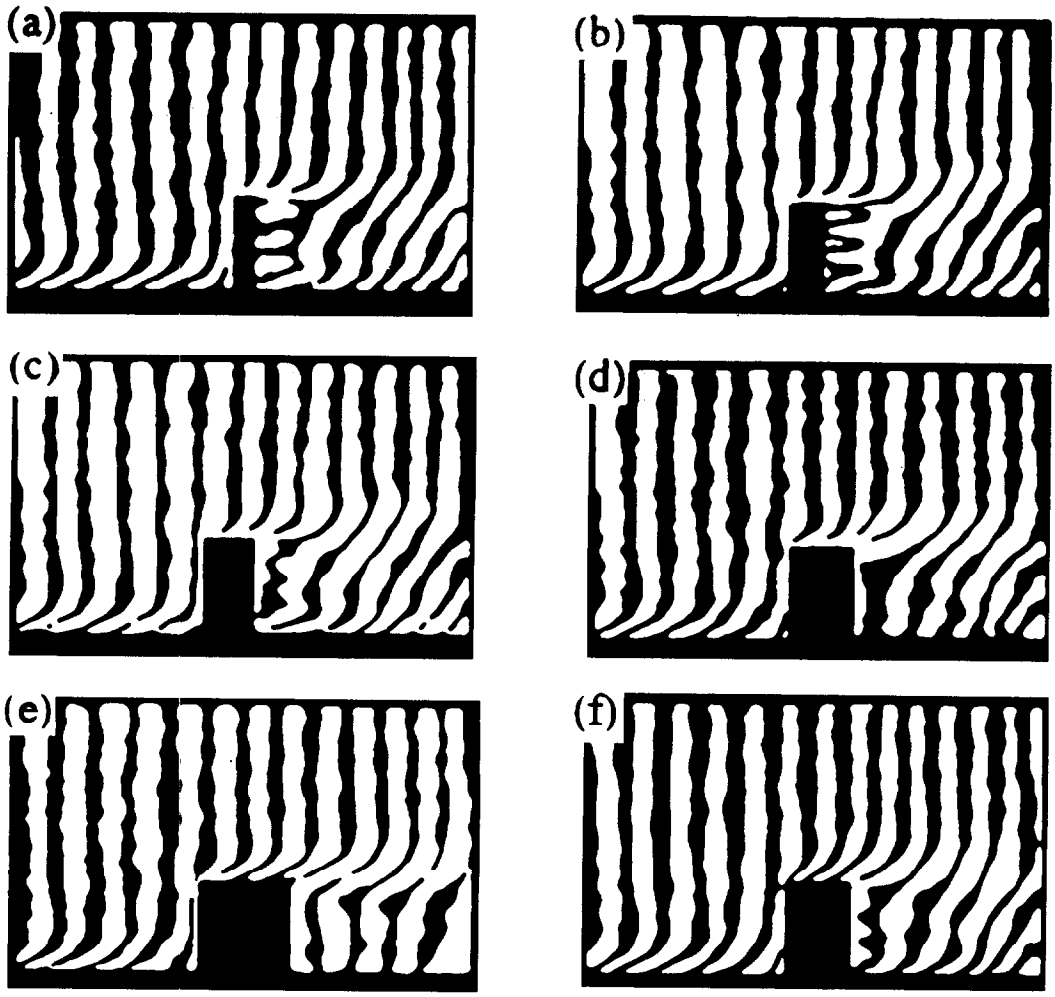

Fig. 1. Typical examples of holographic finite-fringe interferograms: (a) $w/h = 0.16$, $Re = 12\,000$, $\beta = 0.22$; (b) $w/h = 0.35$, $Re = 12\,000$, $\beta = 0.22$; (c) $w/h = 0.5$, $Re = 12\,000$, $\beta = 0.22$; (d) $w/h = 0.7$, $Re = 12\,000$, $\beta = 0.22$; (e) $w/h = 1.0$, $Re = 12\,000$, $\beta = 0.22$; (f) $w/h = 0.7$, $Re = 30\,000$, $\beta = 0.22$.

ous fence open-area ratios are depicted in Figs 4(a) and (b), respectively. At $\beta = 10\%$, the thinnest fence ($w/h = 0.16$), except for the lowest Reynolds number, provides a slightly higher Nusselt number than the solid-fenced geometry [7]. Similar results are also obtained for the fence with $w/h = 0.35$ and 0.5 in a higher Reynolds number range ($Re > 30\,000$). This is because the fences are permeable under these flow and geometric conditions (Fig. 1). It has been verified that the permeable fences could provide a higher heat transfer than the impermeable fences [1, 3]. As the fence open-area ratio increases, there are more data apart from the solid-ribbed correlation. With regard to the fence-thickness effect on the friction factor [Fig. 4(b)], at $\beta = 10\%$, the friction factor for the thinner fence, say $w/h = 0.16$, and 0.35, is significantly lower than that of the wider fence (except for the low Reynolds numbers). Again, as the fence open-area ratio increases, there are more data apart from the solid-fenced correlation [7]. It is concluded that the thinner fences with higher open-area ratios in a higher Reynolds number condition pay the lower friction-loss penalty.

According to the data given in Figs 4(a), and (b), the average Nusselt number and friction factor of the permeable-fenced channel could be inducted respectively into two correlations of $\overline{Nu} = 0.335Re^{0.624}$ and $f = 0.00451\beta^{-0.106}$. Comparing the experimental data with the above correlations, the maximum relative error is less than 7.8 and 9.5%, respectively, for $\overline{Nu}$ and f. Note that both the average Nusselt number and the friction factor are highly dependent on the fence thickness-to-height ratio, although it is not presented explicitly in the above equations. In fact, the fence thickness affects the heat transfer and friction through changing the fence permeability. The procedure of predicting the average Nusselt number or the friction factor of the perforated-fenced channel in terms of the present data is as follows. When the fence geometric and flow parameters (including w/h, β and Re) are given, the fence permeability is determined by Fig. 2 in advance. The average Nusselt number and friction factor are then predicted either directly by the above equations for the permeable fence or by those in the previous article [7] for the impermeable fence.

Figure 5 shows the constant-pumping-power performance of the perforated-fenced channel with various fence thicknesses, which is presented by the relation between $\overline{Nu}/\overline{Nu}_s^*$ and $[f/(0.316Re^{0.25})]^{1/3} \cdot Re$ (denoted as Re^*). To avoid this figure to be over-crowded, the results for some combinations of parameters in Table 1 are omitted. It is seen from this figure, obviously, in the case of $\beta = 10\%$ or in the low Reynolds number region, the thinner fences seem to provide

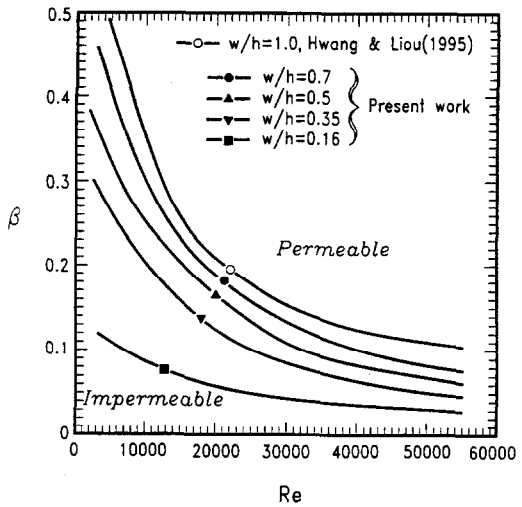

Fig. 2. Effect of the fence thickness on the permeability limit of the perforated fence.

a better thermal performance under the constant pumping power due to their higher permeability.

CONCLUSIONS

The investigation described here, in conjunction with the previous efforts on this subject, has constituted a comprehensive study of the heat transfer and friction characteristics in perforated-fenced channels. During the course of this work, the crucial geometric parameter of fence thickness-to-height ratio, which has never been studied before, is experimentally investigated. The most contribution of the present work is to propose firstly the permeability limit of the perforated fence of various thicknesses. Moreover, it is found that the fence thickness strongly affects the thermal performance through influencing the fence permeability, and the permeability limit of the perforated fence decreases with the decrease of the fence thickness-to-height ratio. For the application of large-scale heat exchangers, regardless of the manufacturing concern, the perforated fences of smaller fence thickness-to-height ratios are recommended for their less material requirement and superior thermal performance.

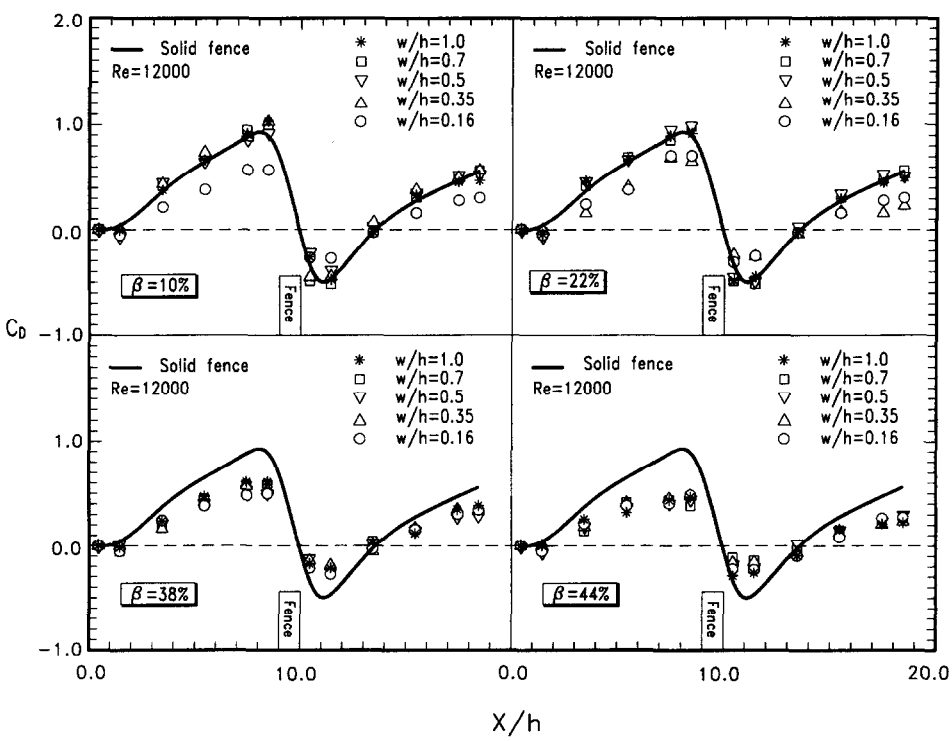

Fig. 3. Effect of the fence thickness on the local pressure drag coefficient distribution along the fenced wall.

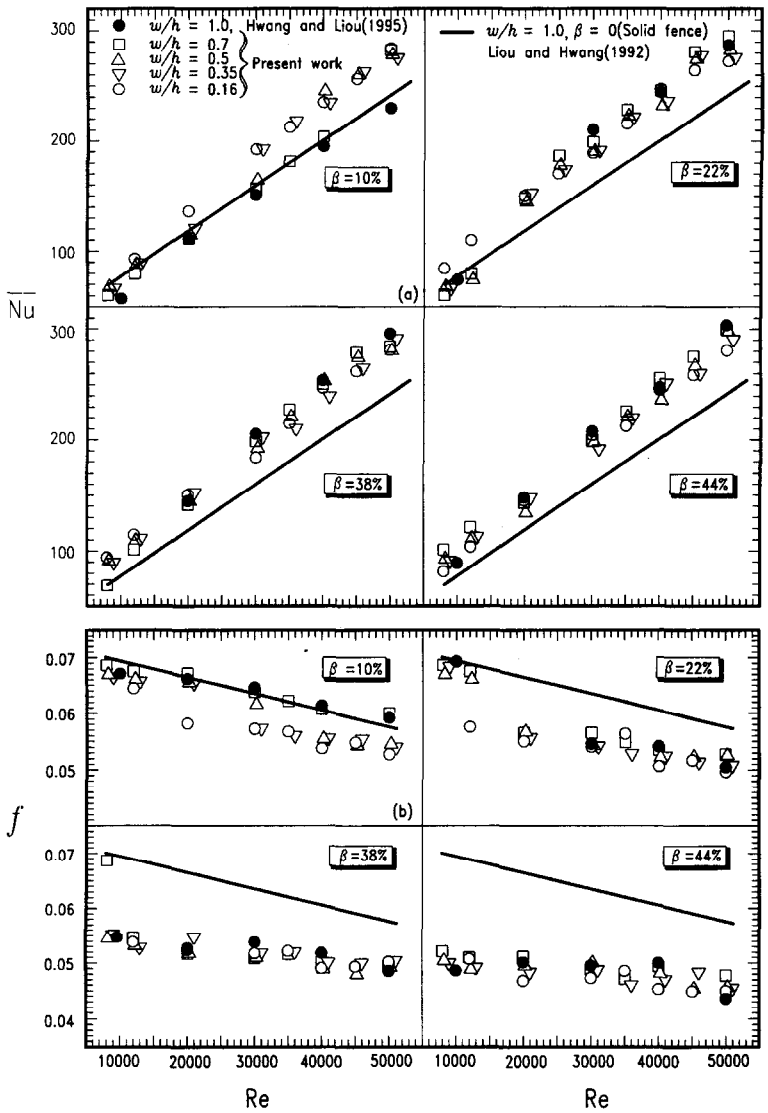

Fig. 4. Effect of the fence thickness on the average Nusselt number and friction factor.

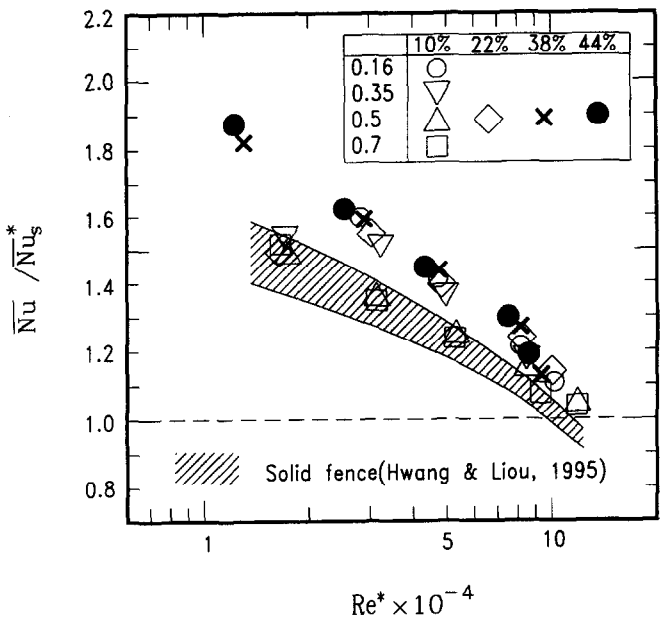

Fig. 5. Pumping power performance for the fenced geometries of various fence thicknesses.

Acknowledgement—Support for this work was provided by the National Science Council of the Republic of China under contract no. NSC 85-2212-E-216-003.

REFERENCES

1. Tanasawa, I., Nishio, S., Takano, K. and Tado, M., Enhancement of forced convection heat transfer in a rectangular channel using turbulence promoters. *Proceedings of ASME/JSME Thermal Engineering Joint Conference*, 1983, pp.395–402.
2. Tanasawa, I., Nishio, S., Takano, K. and Miyazaki, H., High-performance surface for forced-convection heat transfer using novel turbulence promoters, PASME paper, 84-HT-69, 1984.
3. Hwang, J. J. and Liou, T. M., Augmented heat transfer in a rectangular channel with permeable ribs mounted on the wall. *ASME Journal of Heat Transfer*, 1994, **116,** 912–920.
4. Hwang, J. J. and Liou, T. M., Effect of permeable ribs on heat transfer and friction in a rectangular channel. *ASME Journal of Turbomechary*, 1995, **117,** 265–271.
5. Hwang, J. J. and Liou, T. M., Heat transfer in a rectangular channel with perforated turbulence promoters using holographic interferometry. *International Journal of Heat and Mass Transfer*, 1995, **38,** 3197–3207.
6. Liou, T. M. and Hwang, J. J., Turbulent heat transfer and friction in periodic fully developed flows. *ASME Journal of Heat Transfer*, 1992, **114,** 56–64.
7. Kline, J. S. and McClintock, F. A., Describing uncertainties on single-sample experiments. *Mechanical Engineering*, 1953, **75,** 3–8.
8. Stree, R., Watter, G. and Vennard, J., *Elementary Fluid Mechanics*. Wiley, New York, 1976.